

## *Retraction*

# **Retracted: Predicting the Spread of Vessels in Initial Stage Cervical Cancer through Radiomics Strategy Based on Deep Learning Approach**

### **Advances in Materials Science and Engineering**

Received 26 December 2023; Accepted 26 December 2023; Published 29 December 2023

Copyright © 2023 Advances in Materials Science and Engineering. This is an open access article distributed under the Creative Commons Attribution License, which permits unrestricted use, distribution, and reproduction in any medium, provided the original work is properly cited.

This article has been retracted by Hindawi, as publisher, following an investigation undertaken by the publisher [1]. This investigation has uncovered evidence of systematic manipulation of the publication and peer-review process. We cannot, therefore, vouch for the reliability or integrity of this article.

Please note that this notice is intended solely to alert readers that the peer-review process of this article has been compromised.

Wiley and Hindawi regret that the usual quality checks did not identify these issues before publication and have since put additional measures in place to safeguard research integrity.

We wish to credit our Research Integrity and Research Publishing teams and anonymous and named external researchers and research integrity experts for contributing to this investigation.



The corresponding author, as the representative of all authors, has been given the opportunity to register their agreement or disagreement to this retraction. We have kept a record of any response received.

### **References**

- [1] P. K. Pareek, P. A. S. Surendhar, R. Prasad et al., "Predicting the Spread of Vessels in Initial Stage Cervical Cancer through Radiomics Strategy Based on Deep Learning Approach," *Advances in Materials Science and Engineering*, vol. 2022, Article ID 1008652, 13 pages, 2022.

## Research Article

# Predicting the Spread of Vessels in Initial Stage Cervical Cancer through Radiomics Strategy Based on Deep Learning Approach

**Piyush Kumar Pareek,<sup>1</sup> Prasath Alais Surendhar S,<sup>2</sup> Ram Prasad,<sup>3</sup> Govindaraj Ramkumar ,<sup>4</sup> Ekta Dixit,<sup>5</sup> R. Subbiah,<sup>6</sup> Saleh H. Salmen,<sup>7</sup> Hesham S. Almoallim,<sup>8</sup> S. S. Priya,<sup>9</sup> and S. Arockia Jayadhas <sup>10</sup>**

<sup>1</sup>Department of Computer Science and Engineering and Head of IPR Cell, Nitte Meenakshi Institute of Technology, Bengaluru, India

<sup>2</sup>Department of Biomedical Engineering, Aarupadai Veedu Institute of Technology (AVIT), Chennai, TamilNadu, India

<sup>3</sup>Department of Botany, Mahatma Gandhi Central University, Motihari 845401, Bihar, India

<sup>4</sup>Department of Electronics and Communication Engineering, Saveetha School of Engineering, Saveetha Institute of Medical and Technical Sciences, Chennai, Tamil Nadu, India

<sup>5</sup>Department of Computer Science, S. S. D. Women's Institute of Technology, Bathinda, Punjab, India

<sup>6</sup>Department of Mechatronics Engineering, CMR Technical Campus, Hyderabad, India

<sup>7</sup>Department of Botany and Microbiology, College of Science, King Saud University, PO Box 2455, Riyadh 11451, Saudi Arabia

<sup>8</sup>Department of Oral and Maxillofacial Surgery, College of Dentistry, King Saud University, PO Box 60169, Riyadh 11545, Saudi Arabia

<sup>9</sup>Department of Microbiology - Immunology, Northwestern University, Feinberg School of Medicine, Chicago, IL 60611, USA

<sup>10</sup>Department of EECE, St. Joseph University, Dares Salaam, Tanzania

Correspondence should be addressed to  
S. Arockia Jayadhas; arockia.jayadhas@sjuit.ac.tz

Received 10 June 2022; Revised 6 August 2022; Accepted 13 August 2022; Published 28 September 2022

Academic Editor: K. Raja

Copyright © 2022 Piyush Kumar Pareek et al. This is an open access article distributed under the Creative Commons Attribution License, which permits unrestricted use, distribution, and reproduction in any medium, provided the original work is properly cited.

Novel methods and materials are used in healthcare applications for finding cancer in various parts of the human system. To select the most suitable therapy plan for individuals with domestically progressed cervical cancer, robustness metrics are required to estimate their early phase. The goal of the research is to increase the effectiveness of cervical cancer patients' detection by using deep learning-based radiomics assessment of magnetic resonance imaging (MRI). From March 2016 to November 2019, 125 patients with early-stage cervical cancer provided 980 dynamic X1 contrast-enhanced (X1DCE) and 850 X2 weighted imaging (X2WI) MRI images for training and testing. A convolutional neural network model was used to estimate cervical cancer state based on the specified characteristics. The X1<sub>DCE</sub> exhibited high discriminative outcomes than X2<sub>WI</sub> MRI in terms of prediction ability, as calculated by the confusion matrix assessment and receiver operating characteristic (ROC) curve approach. The mean maximum region under the curve of 0.95 was found using an attentive ensemble learning method that included both MRI sequencing (Sensitivity = 0.94, Specificity = 0.94, and accuracy = 0.96). Whenever compared with conventional radiomic approaches, the results show that a variety of radiomics based on deep learning might be created to help radiologists anticipate vascular invasion in patients with cervical cancer before surgery. Based on radiomics technique, it has proven to be an effective tool for estimating cervical cancer in its early stages. It would help people choose the best therapy method for them and make medical judgments.

## 1. Introduction

Exposure to various chemical and physical agents is a typical environmental problem that contributes to cancer mortality. The cervical cancer is the second most common disease in women, with more than half of the million patients are identified every year throughout the globe. Since most instances happen in developing nations and present at an early incurable phase, more than 350,000 people will lost their life as a result of their illness. Every year, around 38,000 patients are reported in Europe, with more than two-thirds anticipated to be treated and live. Survival rates will differ by nation, dependent on treatment centers and, more significantly, whether a screened program has been developed. By reducing the possibility of invasive carcinoma by treating pre-malignant cervical intraepithelial neoplasia before it grows into a really aggressive and dangerous tumor, these approaches will discover the initial phase of illness [1]. Cervical cancer is one of the most prevalent forms of cancer that may affect a woman's reproductive system, and it represents a significant danger to a woman's life and health. The stages of cervical cancer that occur before treatments are required for identifying the available medical treatment choices and for making medical treatment predictions. Tumors that have invaded the parametrium of the cervical canal may only be treated with radiochemotherapy, whereas malignancies of the cervical canal that do not affect the parametrium can be healed surgically. The presence of parametrial enlargement in cervical cancer is connected to an increased risk of recurrence and worse survival following therapy [2].

Penetration of the women cervix infects the cervix deeper tissues. The cervical cancer has the possibility to spread to other functions of the body, including the liver, rectum, bladder, lungs, and genitals. Normal cervical cells grow, reproduce at a certain rate, and then die, causing changes in their DNA. Furthermore, unfavorable cell mutations are exposed, leading to cells violating their control and refusing to die, resulting in the formation of differentiated cells. Abnormal discomfort after intercourse, vaginal bleeding after intercourse, and vaginal discharge after menopause are the most well-known indications of cervical cancer. Figure 1 depicts the various symptoms of cervical cancer. The most widespread risk variables are early sexual activity, multiple sexual partners, compromised immune system, sexually transmitted diseases, and exposure to smoking and miscarriage vaccines [3]. Figure 2 depicts the various risk factors for cervical cancer rising to women. Consequently, accurate diagnosis of cervical cancer with parametrial invasion is important in clinical practice. Conventional magnetic resonance imaging (MR) imaging and gynecological examination are commonly used to evaluate parameter amplification. Traditional imaging characteristics such as full-thickness disruption of normal cervical stroma in T2-weighted images and nodular lesions extending to neighboring parameters were previously thought to be parameter invasion; however, image processing is a standard function. In medical care, an objective

and measurable approach to measuring criterion penetration is required [4].

In 2012, there were approximately 530,000 newly diagnosed cervical cancers and 270,000 deaths worldwide. Undeveloped nations confront the second most common malignancy and the third major cause of cancer death among women. The highest percentages are in Melanesia, Sub-Saharan Africa, Latin America, and the Caribbean. New Zealand, West Asia, and North America have the lowest. Cervical cancer kills more than 92 percent of women in developed countries: 28,000 in Latin America, 60,000 in Africa and 150,000 in Asia. India, the world's second most populous country, accounts for 26% of cervical cancer deaths (70,000 deaths). Cervical cancer is the leading cause of death in women in eastern, central, Melanesia, and southern Africa. Cervical cancer rates vary widely across the country due to variations in access to surveillance, which enables early detection and removal of lesions and the incidence of human papilloma virus (HPV) disease. The prevalence of HPV infection (of all forms) varies explicitly, from 16% in Latin America, 21% in Africa, 5% in North America and the Caribbean to 9% in Asia [5].

As per a WHO report, cervical cancer is most likely the reason of cancer in women in developing countries. Although clinical centers, thousands of extra cases were reported in the United States in 2016, compared to much greater than 20K in 2014. The dataset of cervical cancer provides almost 800 data specimens, 32 features, and 4 targets from the 2016–17 reporting period. Overall traits, tobacco activities, and previous health histories are all important aspects. The abundance of screening and diagnostic procedures, each of which may produce such a diverse set of outcomes, contributes to the complexity of the data. As a consequence of this, determining how the woman's element will behave and selecting the most appropriate screening strategy are both crucial challenges. As a direct consequence of this, the procedure of identifying the most suitable principal channel constitutes the primary obstacle in the endeavor of measuring a woman's exposure to risk factors. A lot of academics have looked at data on cervical cancer that was compiled from a variety of different sources. The major risk factors for the spread of cervical cancer include improper menstrual hygiene, having children at a young age, smoking, and a lack of preventative measures for mouth cancer. The tumor phase, initial weight mass, and histological grading are all variables that affect the prediction. Therapy is made up of four phases of illness as established by the International Federation of Gynecology and Obstetrics (FIGO) scoring scheme. Surgery or radiation therapy is utilized to handle patients with stage IIA or less. Initial stage cancer patients may need a radical hysterectomy, radiation treatment, or sometimes both. People diagnosed with stage IIB or higher, on the other hand, receive only radiation therapy. Stage IIA disease without stage parametrial involvement and stage IIB disease, in which parametrial involvement are the main difference in stages. Figure 3 represents the different stages of

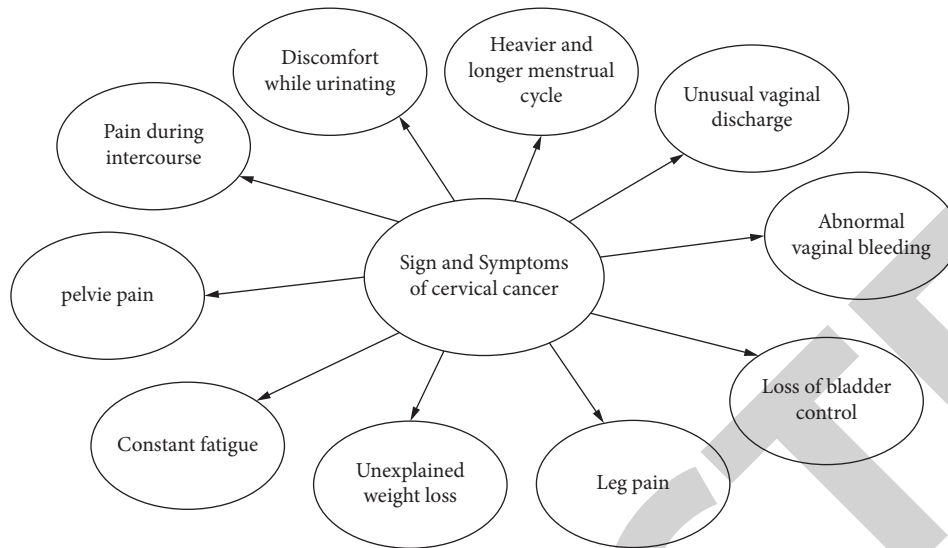


FIGURE 1: Basic symptoms of cervical cancer.

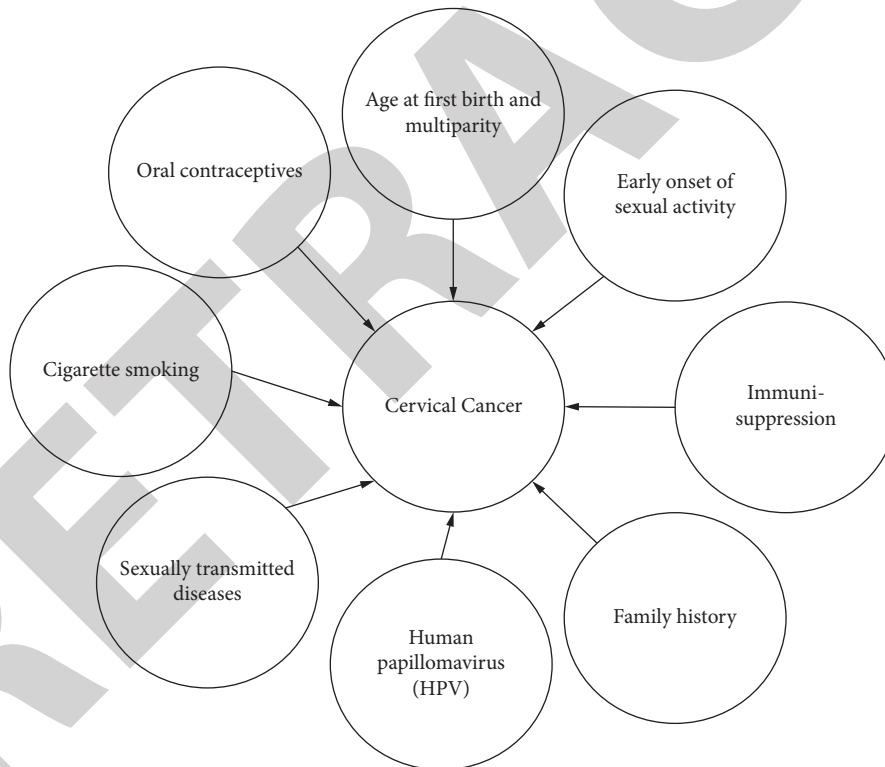


FIGURE 2: Various risk factors for cervical cancer.

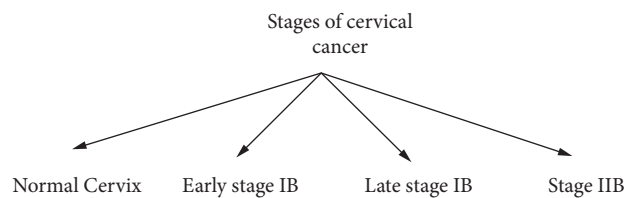


FIGURE 3: Different stages of cervical cancer.

cervical cancer. Although lymph node metastasis is not comprised in the formal FIGO scoring system, they are an important prognostic factor. The TNM staging approach to cervical cancer involves nodal status. Unilateral and bilateral parameters are other prognosis variables for the occurrence of pelvic wall disease [6].

The size of the tumor at prognosis, the size of the high-risk clinical objective during bronchial therapy, and the duration of therapeutic effects are linked to the potential of local democracy. Furthermore, in the epoch of image-guided responsive therapy, it is essential to check the outcome evaluation, especially for those at significant risk of local recurrence, and to intensify medication (or) radio sensitizing Agent who is applicants for clinical trials. On the other hand, identifying individuals at low risk of local recurrence may be clinically important. Clinical imaging is essential in the primary assessment and condition of victims and in the treatment of treatment options. Because of its great resolution, functional imaging capabilities, and excellent soft-tissue contrast magnetic resonance imaging (MRI) is the gold typical for the pre-treatment evaluation of gynecologic malignant T-status [7]. Radiation therapy and concurrent chemotherapy with cisplatin-based chemotherapy is a standard therapy for women with metastatic cervical cancer, as per the NCCN recommendations; the 5-year life expectancy can approach 60–80 percent. If first-line CCRT failed, though, the longer CCRT therapy time will unavoidably delay the start of other possibly beneficial therapies. Furthermore, CCRT has several adverse effects. Additional pelvic irradiated can induce myelosuppression because it damages the bones, which comprise more than 50% of the body's proliferative functional bone marrow mass. Platinum-based CCRT can worsen myelosuppression, although it is less effective if therapy is initiated or interrupted. As a result, predicting CCRT responsiveness before therapy may help to determine whether CCRT should be used as first-line therapy. Furthermore, by identifying individuals who are most susceptible to CCRT, responder prognosis can lead to individualized therapy [8]. Figure 4 describes the treatment option available for cervical cancer.

The Ministry of Health of Bangladesh has launched the 5-year national approach for family welfare cervical cancer control and prevention Initiative, which will run from 2016 to 2021. The WHO considers invasive cervical cancer to be the fourth most widespread and second leading cause of cancer among Bangladeshi women aged 20 to 50 years. Each year, approximately 12,000 new cases are identified, and the severity of the condition exceeds 6,000. In Bangladesh, nearly 4.4 percent of the general population has a higher risk of developing cervical HPV16/18 infections at any given time, and HPVs 16 and 18 are responsible for 80.3 percent of invasive cervical malignancies [9]. Figure 5 depicts the mortality rate of cervical cancer during the year from 1990 to 2020. Targeted treatment requires imaging. Radiomics collects huge volumes of information from high-performance clinical pictures to extract attributes for unbiased, measured investigation of diseased biological activities [10]. Radiomics have been intensively explored in tumor

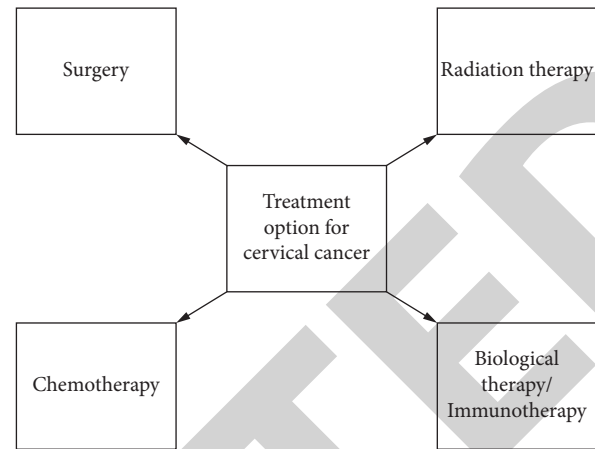


FIGURE 4: Treatment option available for cervical cancer.

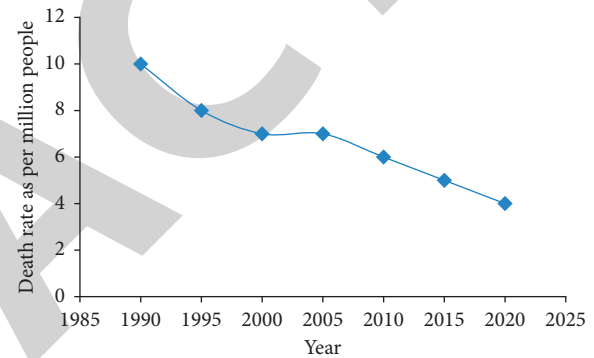


FIGURE 5: Mortality rate for cervical cancer from 1990 to 2020.

detection, differentiated diagnostic tests, prognostic assessment, and therapy outcome prediction in recent decades. This approach has been used to estimate LNM in breast cancer, bladder cancer, biliary tract cancer, and colorectal cancer before surgery [11]. Some research has looked at the effectiveness of radiomics in calculating LNM in cervical cancer. The radiomics properties of positron emission tomography (PET) were linked to the expression of VEGF in cervical cancer in a prior study. This observations suggest that a radiomics system based on health images may be used to predict VEGF expression [12].

Radiomics is a novel approach for obtaining high-throughput data from normal clinical pictures. The radiomics nomogram was used to identify LNM status by collecting measurable characteristics from CT images connected to colorectal, bladder, esophageal, breast, lung adenocarcinoma, and thyroid. It functioned well [13]. Radiomics is a rapidly expanding field of science that uses image collections of high-dimensional characteristics taken from routinely obtained cross-sectional images to produce data that semantic assessment would otherwise lose. Radiomics records the cystic and necrotic patches within the tumor volume that are typical of tumoral heterogeneity, as well as behavior that characterizes aggression and therefore results. Radiomics is an area of research that uses mathematical modeling to extract qualitative information from

clinical images in order to create prediction methods that may be used to estimate treatment prognostic and survivability, with preliminary results reflecting a wide range of medical results [14].

In comparison to nonmedical databases, healthcare sets of data feature more attributes and partial information. This is critical to establish the essential and useful properties for quantified approach building by enhancing type. Although deep learning approaches are stronger in forecasting and effective tweaking, they have been frequently utilized in cancer research. An investigation found that long-term HPV infection is the main reason for cervical cancer [15]. Machine learning is a technique that leverages previously established diagnosing characteristics as factors, such as morphological or textures, and needs factors pre-selected by people to do categorization jobs. Deep learning, on the other hand, retrieves whatever the system defines as essential factors directly from the training phase, avoiding the preconceptions that come with past human analysis. This will eventually offer physicians with methods that will aid in the proper detection of cervical cancer [16]. In this study, deep learning-based VGG19network is used for the early detection of cervical cancer.

## 2. Related Works

Imaging-based tumor size predicts cervical cancer radiation response before, during, and after treatment. Various imaging-based tumor size measurement approaches and time have not been examined. To compare the diagnostic usefulness of orthogonal diameter-based elliptical tumor volume measurement vs. contoured tracing evaluation 3D tumor volumetric. 60 patients (stages IB2-IVB/recurrent) with advanced cervical cancer underwent continuous MRI exams throughout early RT, mid-RT, and follow-up. In the computer workstation, the measurement based on ROI was calculated by monitoring the whole tumor area on each MR piece. Three orthogonal diameters ( $a_1$ ,  $a_2$ ,  $a_3$ ) were determined on image hard copies to calculate the volume as an ellipse for the diameter-based "elliptical volume". These results were compared between the two measurement techniques, and the series tumor sizes and regression rates calculated with each approach were linked to local management, disease, and survival time. The average duration of treatment was 5 years. A mid-treatment MRI scan using 3D ROI volumetry is the best approach and time point for estimating tumor size to predict tumor regression rate. Both the diameter-based technique and the ROI measurement had to predict accuracy equivalent to pre-RT tumor size, especially in patients with small and large RT tumors. Tumor size prior to RT was determined by any approach and, on the other hand, showed a significantly lower prognostic value for intermediate-sized tumors that accounted for most patients. The largest result of predicting local control and disease survival rates is the tumor regression rate gotten during mid-RT, which can only be recognized by 3D ROI measurement. Slow ROI-based regression rates were predicted within the difficult intermediate pre-RT group to classify all treatment complications. The results were not predicted by the mid-RT

regression rate depend on the base diameter measurement. Of all the measurement methods, the initial-RT and post-RT measurements were the least informative. The first findings show that a simple diameter-based estimate obtained from film hardcopy can be used to determine the initial tumor size for the treatment performance prognosis in cervical cancer. When the initial tumor size is intermediate, ROI measurement and additional MRI are required during the RT to objectively measure the tumor regression rates for clinical outcome evaluation. The baseline diameter-based approach of this study is not optimal for evaluating the response throughout treatment [17].

Cells usually split and expand to make additional cells only if the body requires them. Whenever new cells are not required, this ordered procedure keeps the process going. Those cells may produce a cancer progression, which is a mass of excess tissues. Effective data processing methods are used to diagnose whether the cervix is normal or cancerous. With the help of powerful data processing methods, normal cervical or cancer cervical prognosis is calculated in this study. Predictive data processing is important, especially in the medical field. The regression and classification tree system, the K-learning with Random Forest Tree algorithm to predict a usual or cancerous cervix are all based on this principle. Information was analyzed from NCBI and utilized from a data collection with 500 samples and 61 parameters. The results were shown in the format of predictive trees. As previously indicated, a sample of 100 data with 61 biopsies characteristics was chosen. Depending on the biopsies results, an awareness program is implemented, and a questionnaire is undertaken to track women's changes over this time. A personalized interviewing program was done amongst rural women in diverse locations to obtain data effectively. Patients were screened for cervical cancer in collaboration with JIPMER Hospital. The findings of the biopsy tests were statistically analyzed and submitted to MATLAB for algorithmic verification. To determine the results obtained, 100 test datasets and 60 training packages are divided and presented in different heads. To find the best cervical cancer prognosis, the researchers compared the effectiveness of several methods using measures such as sensitivity, specificity and accuracy. The regression approach was initially used to make predictions. Normal cervical or cancers cervical is two possible side effects of CART binary tree. The GINI index is a separation criterion used to determine the different types of cervical information. After the RFT confirmed the optimal accuracy, a new logic was adopted, namely "mixtures of two techniques." This is the supervised machine learning group approach. To create the best predictive effect, whitening is utilized as a pre-process in the k-mean cluster. With the CART TREE result, the findings represent 83.87 percent accuracy. To increase forecast efficiency, Random Forest Tree (RFT) is used. To achieve 93.54 percent forecast efficiency using the MATLAB code. Because the K-Means method is useful for estimating datasets, the RFT - K- i.e. learning tree output achieves high accuracy. This approach is unique in that it combines RFT with the K-means method, resulting in a greater accuracy result. This algorithm has been ineffective for the exact prediction of cervical cancer [18].

Prevention methods are cheaper than medical treatment in practically all countries. The primary diagnosis of any disease improves the chance of effective treatment for patients rather than the disease diagnosed late in its course. Cervical cancer is caused by a variety of factors, including aging and the use of hormonal contraceptives. Cervical cancer can be diagnosed early, which increases healing and reduces mortality. The study use machine learning methods to improve a method that can precisely and sensitively diagnose cervical cancer. The categorization approach was constructed using the cervical cancer potential risk database from the University of California at Irvine (UCI) using a polling approach that included three classification techniques such as decision tree, random forest and logistic regression. To solve the difficulties of asymmetric learning and to decrease the variables that do not disturb the accuracy of the sample, the Minority Surface Model (SMOTE) integrated with the Primary Component Analysis (PCA) approach was used. The excessive fitting problem was avoided using the 10-fold cross-verification approach. The database contains 32 risk factors and four targeted variables (Hinselmann, Cytology, Schiller, and Biopsy). The study found that combining voting classifiers with SMOTE and PCA approaches improves the sensitivity, accuracy, and area of prediction models under the ROC for each of the four target variables. For all target variables, the SMOTE-voting approach increased accuracy, sensitivity and PPA ratios from 0.9 percent to 5.1 percent, 39.2 percent to 46.9 percent, and 2 percent to 29 percent. Furthermore, the PCA technique improved sample performance by eliminating computational processing time. Lastly, after comparing the findings to those of multiple prior research, study exposed that these models were more efficient in identifying cervical cancer based on key assessment criteria. In this method, the correct prediction of the original feature is difficult [19].

Another study looked at and proposed an effective and enhanced cervical cancer forecasting model. Previous monitoring and detection methods/tests were complex, time-consuming, and clinical/pathological. Machine learning predicts and diagnoses cervical cancer. For measuring performance in illness diagnosis, an integrative technique of Adaptive Boosting and Genetic Algorithm is applied. To reduce the amount of features, a genetic algorithm is utilized as feature selection. It minimizes both the computing price and the number of components required for diagnosis. Adaptive Boosting is a technique for improving classifier performance. For illness identification, the Support Vector Machine (SVM) and Decision Tree are recommended. For cervical cancer detection, 32 variables are utilized. The set of variables is decreased using a genetic approach, and adaptive boosting is recommended for additional improving performance. For the radial bias function of support vector machine, decision tree, and SVM linear, the improvement in accuracy was 94 percent, the sensitivity was 97 percent–98 percent, the specificity was 93 percent–94 percent, and the accuracy was 93 percent–95 percent. A combined method of adaptive promotion and genetic mechanism is suggested. It requires more time for processing and exact prediction is difficult for the high-noise image [20].

Cervical cancer is the most leading cause of mortality, especially in developing countries, although it may be efficiently managed if identified earlier. The goal of this work was to create effective machine-learning-based classification models for early-stage cervical cancer detection utilizing clinical studies. The study used a Kaggle data repository cervical cancer databases that had four different types of aspects including cytology, Hinselmann, biopsy, and Schiller. Those class characteristics were used to divide the database into four groups. This dataset was subjected to three feature modification methods such as sine function, log and Z-score. The performance comparison of many supervised machine learning methods was evaluated. For the biopsies and cytology data, the Random Tree (RT) method performed best, while Random Forest (RF) and Instance-Based K-nearest neighbor (IBk) performed best for Schiller and Hinselmann correspondingly. The logarithmic transformation approach to the biopsy dataset worked best, while the sine function worked best for cytology. The Hinselmann database performed well on both logarithm and sine functions, while the Schiller database performed well with the Z-score. Multiple feature selection techniques (FST) approaches have been used for modified datasets to identify and prioritize related risk variables. The findings of this study show that clinical evidence, tuning and relevant computer structure, classification, and machine learning approaches can be effective and accurate. Diagnose cervical cancer in its early stages. This method is inefficient and difficult to predict the exact value [21].

Health care providers are now confronting a significant problem in recognizing cervical cancer before it progresses fast. To access the risk variables for predicting cervical cancer by using machine learning classification algorithms. Effective variation of the eight most categorical algorithms for diagnosing cervical cancer using various excellent features selected from the database. Machine learning classifiers such as Decision Tree, Multilayer Perceptron (MLP), K-Near Neighbor and Random Forest, Logistic Recursion, Gradient Boosting, Adaboost, and SVC are help to identify the early detection of cervical cancer. To prevent values from disappearing in the database, several procedures are used. A mixture of selecting features approaches including SelectBest, Random Forest, and Chi-square was used to select several excellent properties. Recall, accuracy and f1-score properties are utilized to evaluate the effectiveness of classifiers. MLP outperforms other classification techniques in the range of best-selected features. At database segmentation rates, most classification techniques claim to have the greatest accuracy in the first 25 characteristics. The ratio of correctly classified examples to each sample is shown, and all of the findings are analyzed. Medical practitioners can carry out cervical cancer prediction in an effective manner by using the recommended method. This method has a cumulative loss function, making it difficult to predict cancer [22].

To examine whether strain elastography imaging can be used to diagnose and predict treatment outcomes in patients receiving simultaneous chemo-radiotherapy (CCRT) for locally advanced cervical cancer. In a 2015–2016 feasibility assessment, 47 individuals with advanced localized cervical cancer were registered. All patients had CCRT and filtered elastography before, one week, two weeks, and immediately



after therapy. MRI was used to evaluate treatment response during diagnosis and following CCRT. Depending on the MRI findings the outcome of treatment can be classified as a full response, partial response, chronic disease or progressive disease. Clinical results have been compared with the rate of strain of normal parametrial tissue and cervical tumor. Of the 47 patients who completed all four exams, 36 were evaluated: 25 were categorized as CR, 11 as PR and 0 as SD/PD. The CR group ( $F=87$ ) and the PR group ( $F=38$ ) had significantly different strain ratios at different time periods. The CR and PR sets had considerably different strain rates ( $F=7.2$ ). At 1 week of treatment, the strain rates in the CR and PR collections varied considerably ( $p 0.05$ ). Week 1 and 2, and post-treatment (all  $p 0.001$ ) showed a significant decrease in the CR group, whereas week 2 and after treatment (both  $p 0.05$ ) showed a significant decrease in the PR group, but not at week 1 during CCRT. A prospective combination study was performed to estimate cancer response in women who getting CCRT for cervical cancer. The work demonstrates the ability of strain elastography imaging to monitor and predict tumor response developed by CCRT [23].

### 3. Materials and Methods

**3.1. Data Collection.** Samples of 1500 diagnostic MRI images were collected from an average of 150 female patients aged 55 years and above in online databases of international collaborations on cancer reporting over a period of 30 to 65 years between March 2016 and November 2019, with 600 naval invasions and 900 non-naval invasions. In each case, two MRI methods were captured such as  $X1_{DCE}$  MRI, which focused on anatomical features and efficiently measured blood flow in vivo; and  $X2_{WI}$  MRI, which stronger the contrast of the soft tissues. Patients with  $X1_{DCE}$  and  $X2_{WI}$  MRI assessments prior to surgical treatment; Surgical extraction cases with pathological verification utilized as the typical gold for distinguishing non-invasive and vessel invasion properties of cancer; And all women over 20 years of age were included. Individuals with a history of preoperative treatment, women with no  $X1_{DCE}$  or  $X2_{WI}$  MRI data, women with no histopathological effects, patients receiving congenital therapies, and very young patients with cases of other cervical diseases or tumors were excluded. A radiologist with 10 years of expertise used 4.0-T scanning with sensitive coded abdominal scrolls of 8-channel arrays to perform preliminary MRI examinations. Before screening these individuals were told to drinking some water to fill their bladder, rest taken for 30 minutes, and bring their respiration under control. Clinical records were reviewed to collect patient data such as patient age, menstrual status, international gynecology and obstetrics stage and tumor type, LN and lymph vascular space invasion histological findings after surgery. Table 1 shows the patients' various characteristics for training and testing phase.

**3.2. Data Image Preprocessing.** Each  $T1_{DCE}$  and  $T2_{WI}$  image was examined using the ITK-SNAP program by MRI radiologists with 10 and 12 years of experience. The ROI per patient was created at an average range of  $30 \times 40$  pixels per image and

included tumor areas and borders of cervical cancer located in the cervix. The ROI patch from each MRI image was automatically generated and measured at  $256 \times 256$ , and then fed into in-depth learning networks. Data augmentation was utilized to train the convolutional neural network models and balanced the datasets using the image data generator of the Keras module in Python 3.9. Every image is initially measured and cut before being moved up and down, before being moved to right from left, and then arbitrarily interchanged 6 degrees around the midpoint. It was thought that pixels beyond ROI could carry important information for discrimination because cervical tumor cells travel to neighboring healthy tissues in patients with vascular invasion. To compare ROIs, the array of pixels from the minimum boundary rectangle (MBR) is stretched at different positions (top, bottom, left, and right). The produced images were enhanced with data amplification utilizing the same technique before being placed on the network's input layer. Figure 6 depicts the process flow diagram for cervical cancer prediction.

**3.3. Convolutional Neural Models for Classification.** CNN, also known as convolutional networks, was employed as direct inputs to the network instead of feature representation, unlike standard radiomic techniques. The algorithm is a self-sufficient gathering and improvement of advanced traits and variables. MRI scanned regions from cervical victims were used as inputs for the end-to-end convolutional networks model in this study. The output layer of each strategy was constructed to comprise two neural networks to predict the possibility of with or without ship incursions. Several CNN techniques, including VGGNet, GoogLeNet, Residual Network, and DenseNet, have been used to analyze various radiomic processes. More detailed explanations may be found in the source articles for each CNN model.

In order to adapt to this work during the experiments, the first fully connected components in every neural network were exchanged with three additional entirely connecting layers with a neural number of 700, 500, and 5, respectively. Adam optimizer and cross-entropy losses were used to train all networks with a detection rate of 0.0002. During each Conventional blogging of AdaptedVGG19 networks, a custom compression and trigger mechanism and components of the Convulsion Block focus were added to create an AdaptedVG1919-SE and AdaptedVG1919-CBAM accordingly. The two separate AdaptedVGG19-focused network integrated judgments were used to develop a deeper group learning approach and an observational group learning approach accordingly.  $D = (d1 + d2)/2$  was used to calculate the output probability of becoming a ship invasion or non-ship invasion, where  $d1$  and  $d2$  reflect the effect potential of two AdaptedVGG19 networks using  $X1_{DCE}$  and  $X2_{WI}$ . Figures 7 and 8 represent the architecture model for suggested VGG19 approaches and its inner structure processing.

**3.4. Mechanism for Validity.** The effectiveness of the radiomic algorithms was evaluated using 10-fold cross-validation, and the accuracy, sensitivity, and specification were calculated using the calculations below. The amount of



TABLE 1: A selected patient training and testing phase attributes.

Patients characteristics	Training phase N= 150			Testing phase N= 55			<i>p</i> -value	<i>p</i> *-value
	+ive lymphovascular invasion	-ive lymphovascular invasion	<i>p</i> -value	+ive lymphovascular invasion	-ive lymphovascular invasion	<i>p</i> -value		
Patients age/year			0.60			0.53	0.98	
Average age	55	56		53	60			
Age ranges	27–55	27–60		30–55	35–65			
Stages			0.62			<0.0002	0.45	
Early stage IB	20 (50.2)	40 (52.6)		15 (30.4)	35 (70.2)			
Late stage IB	15 (42.5)	48 (50.1)		18 (40.2)	20 (40.2)			
Stage IIB	8 (18.5)	12 (13.2)		12 (52.6)	8 (10.2)			
MRI lymph node status			<.002			0.002	0.70	
Positive	20 (7.9)	30 (40.2)		10 (55.2)	50 (92.1)			
Negative	150 (95.7)	52 (68.2)		12 (60.8)	15 (20.5)			
Menstrual status			0.542			0.442	0.89	
Postmenopausal	15 (40.3)	55 (56.2)		6 (30.2)	30 (52.7)			
Premenopausal	28 (65.2)	48 (50.2)		15 (80.5)	35 (56.8)			
Maximum cancer diameter			0.002			0.008	0.55	
≤5 cm	25 (60.2)	80 (88.5)		8 (52.8)	42 (68.5)			
>5 cm	20 (45.6)	18 (17.06)		10 (54.8)	9 (15.9)			
Lymphovascular invasion			<.002			.001	<.002	
Positive	88 (35.9)	46 (59.8)		18 (22.6)	15 (35.9)			
Negative	170 (59.8)	35 (40.8)		97 (89.0)	28 (70.2)			

disorder cases properly identified is represented by True Negative ( $t_n$ ) and True Positive ( $t_p$ ). The quantities of disorder cases incorrectly identified were labeled as False Positive ( $f_p$ ) and False Negative ( $f_n$ ).

$$\begin{aligned}
 \text{Accuracy } (A_c) &= \frac{t_n + t_p}{f_n + t_n + f_p + t_p}, \\
 \text{Sensitivity } (S_n) &= \frac{t_p}{f_n + t_p}, \\
 \text{Specificity } (S_p) &= \frac{t_n}{f_p + t_n}.
 \end{aligned} \tag{1}$$

This method's capacity to distinguish between non-vessel invasion and vessel invasion events is reflected in its efficiency. To refer specificity to a model's ability to appropriately distinguish non-vessel invasion. Sensitivity refers to the model's ability to properly distinguish vessel incursion. The median receiver operational characteristics assessment and the area under the ROC curves were also used to assess these approaches. A confusing matrix was created using the Scikit-Learn module to evaluate the classification performance of the suggested approaches. The gradient-weighted glass activation mapping approach was used to create the heatmaps. Algorithm 1 shows the deep learning-based radiomics strategy for cervical cancer prediction.

## 4. Results and Discussion

### 4.1. Performance Classification in Various Configurations.

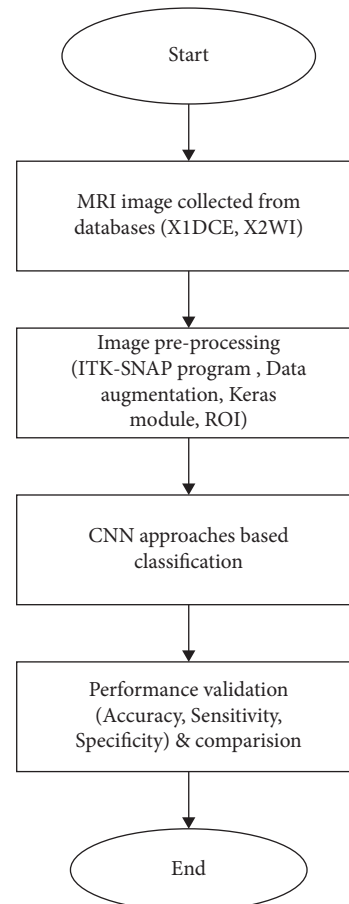


FIGURE 6: Cervical cancer prediction step by step procedure.

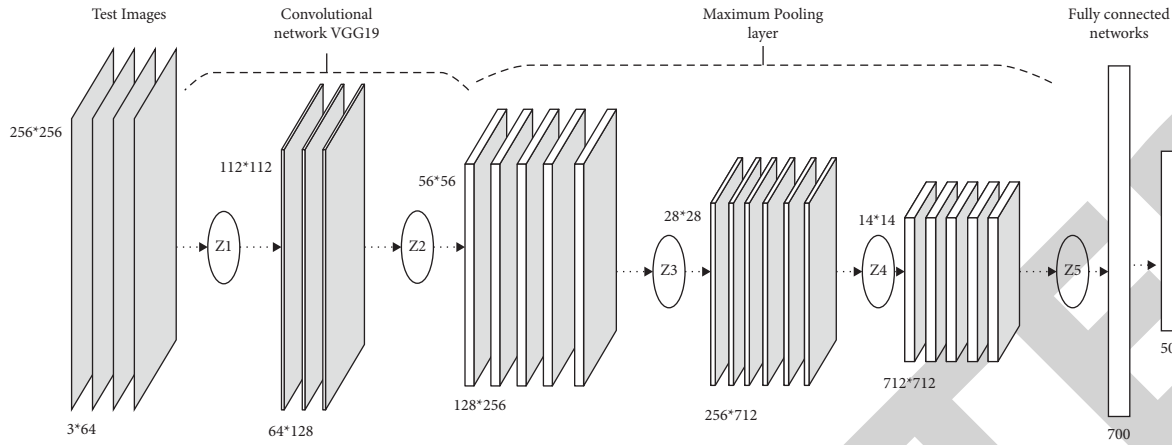


FIGURE 7: Schematic diagram for suggested adaptive VGG19 approach.

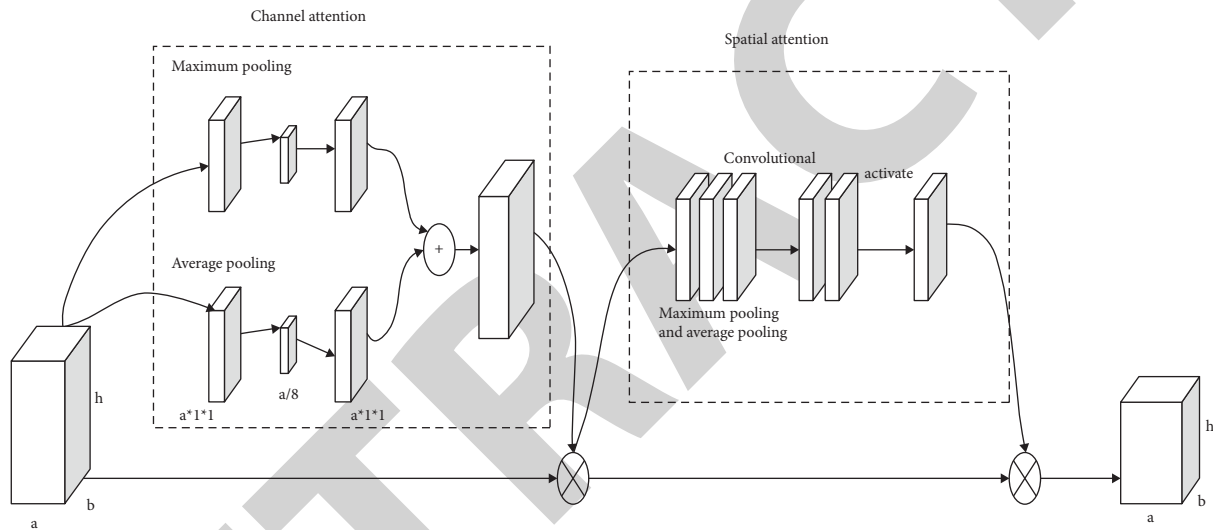


FIGURE 8: Inner structure process flow diagram for adaptive VGG19.

Current studies have found that combining data from multiple methods increases discriminatory performance compared to using individual methods. Since both the  $X1_{DCE}$  and  $X2_{WI}$  MRI datasets provide rich and varied signal intensity within the cancer, Convolutional neural network-based radiomic algorithms were developed in this work. The effectiveness of the approach for vessel invasion discriminations is shown in Table 1. Findings of each model are presented, including AUC average value, sensitivity, accuracy, and uniqueness. As seen in Table 1,  $X1_{DCE}$  consistently defeats  $X2_{WI}$ , proving that the  $T1_{DCE}$  database is more valuable than the  $X2_{WI}$  database. Furthermore, the sensitivity determined by  $X2_{WI}$  for every scenario was lower than that produced by  $X1_{DCE}$ , showing significant error rates by  $X2_{WI}$ .

The primary cause of  $X1_{DCE}$  MRI is the ability to effectively estimate blood flow in vivo by displaying blood vascular density and permeability, estimating the capacity transmission constant, and depending on the permeability of the cancer vasculature, all of that can give more discriminating data on the prognosis of cervical cancer vessel invasion.  $X2_{WI}$

provides anatomical data by screening soft tissues with high resolution to reveal tumor morphological characteristics. Furthermore, current findings are difficult to describe because there are no specific indicators to identify the quality of vascular infiltration in cervical cancer using preoperative MRI imaging. Compared to ResNet-v2, Inception-v3, and DenseNet, the AdaptedVGG network generated improved accuracy and AUC values for  $X1_{DCE}$  and  $X2_{WI}$  databases. Based on the small ROIs collected from MRI images, the most basic topologies of the AdaptedVGG network can be useful in minimizing excess compatibility with sophisticated structures compared to other CNN models.

The remaining designs were said to allow greater accuracy in diagnosing clinical images, which contradicted the findings. This can be calculated based on AdaptedResNet50 and AdaptedVGG19, which have 80,402,590 and 84,922,700 training variables, correspondingly. AdaptedcResNet performed worse than AdapedVGG19, which may be due to greater compatibility. In terms of information size and modeling ability, there has to be a compromise. When the information set is large enough to effectively train a large

```

Input: Test MRI images from datasets
Output: Prediction of the cervical cancer (normal cell (or) abnormal cell)
Initialize the number of specimen (Ns), tumor length (Lt), Image processing (Ip)
While (not satisfied the termination condition)
  for  $i$  ranges (0, Ns)
    Randomly selected the specimen N1, N2, N3. ....Ns then perform the operation
      for  $j$  ranges (0, Lt)
        If  $\text{rand}(0, 1) < \text{rand}(0, Lt) == j$ 
          Perform the image processing operation
        else
          Do not perform the image processing operation
        end if
      Get the new image (Nsn)
    end for
  end for
  for  $i$  in range (0, Ns)
    If tumor volume (Nsn) > tumor volume (Ns)
      Update cancer state (normal/abnormal)
    else
      Not update cancer Ns
    end if
  end for
end while

```

ALGORITHM 1: Deep learning-based Radiomics strategy for cervical cancer prediction.

model, the structure is more likely to perform better. Excessive fit, on the other hand, can be frustrating when the information is too large to sustain training. The small number of photos in our investigation may have had an impact on the effectiveness of the models. The optimum AUC of 0.880 was achieved by combining the results of the  $X1_{DCE}$  and  $X2_{WI}$  databases using the deep group learning approach. The craft properties used to predict vascular invasion status using  $X1_{CE}$  MRI created a radiomics nomogram approach and a current of 0.95 AUC before trial. Similarly,  $X2_{WI}$  used MRI to capture craft properties and developed a logistic regression model with 0.710 AUC.

The maximum AUC in this test reached 0.911, which uses the recommended ensemble technique, which combines both MRI methods. This was in line with previous research that focuses on distinguishing the capabilities of the network and enhancing categorization capabilities. The SE component used in this study can lift the weight of the attributes of the most essential channels. Integrated channel attributes and spatial dimensions data were central to CBAM components. These findings suggest that careful group methods may be useful in predicting vascular invasion in cervical cancer. If the ROC curves are combined with false positive and true positive ratios, a more complete outcome can be obtained.

For such an  $X1_{DCE}$  MRI, as shown in Figure 9 performance evaluation, the curvature of the  $X1_{DCE}$  and  $X2_{WI}$  models is always greater than that of other structures.  $X1_{DCE}$  &  $X2_{WI}$  worked better than AdaptedVGG16. This demonstrates that CNN models of various depths can learn features from various levels and that networks with multiple layers performed somewhat excellent than those with lower levels. Considering the better

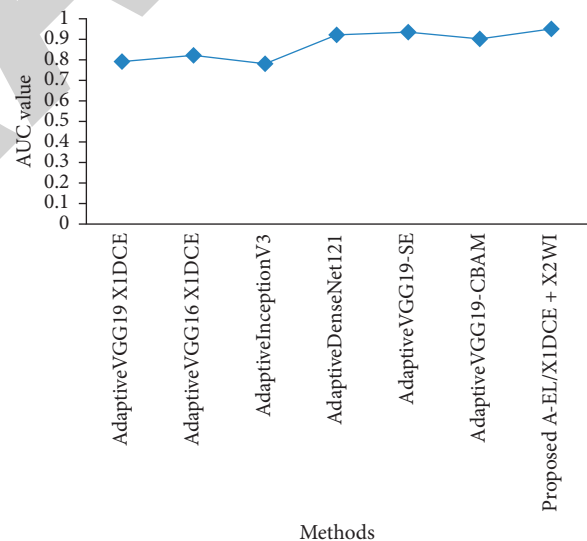


FIGURE 9: Various technique performance evaluation by using receiver operating curve.

specification, AdaptedResNet50-v2 quickly surpassed AdaptedInception-v3 and AdaptedDenseNet121. Adapted Inception-curve, on the other hand, v3s are generally lower than others. Similar findings were made for  $X2_{WI}$  MRI in predictive performance, with the exception of AdaptedResNet50-v2. The study shows the ROC curve of EL modeling combining  $X1_{DCE}$  and  $X2_{WI}$  data, which is an optimal average AUC of 0.95. Figures 10 and 11 depicts the different technique evaluation for predicting the accuracy and sensitivity.

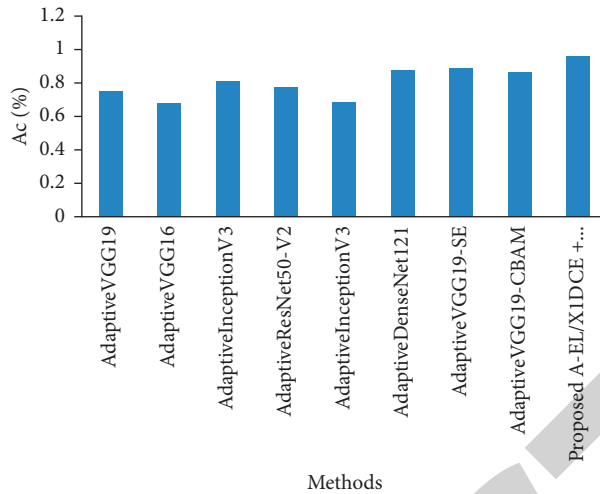


FIGURE 10: Different approaches to accuracy prediction.

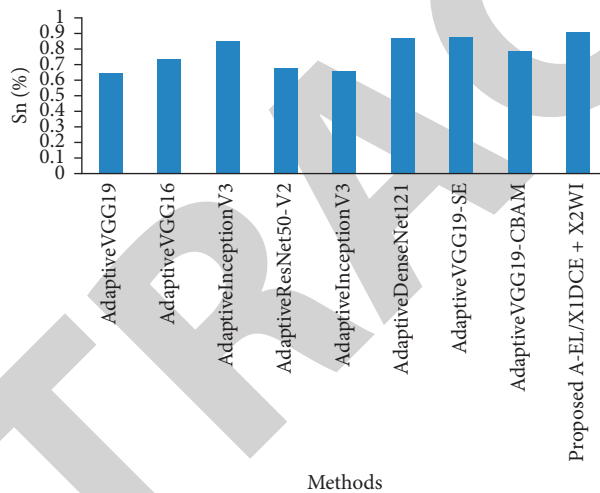


FIGURE 11: Different approaches to sensitivity prediction.

4.2. *The Peri-Tumor Area’s Effect on Estimating Vessel Invasion.* Tumor cells can spread to the pelvic area where they can travel to the blood or lymphatic vessels and other human tissues, leading to invasion and metastasis of cervical cancer. To test the discriminatory ability of peri-tumor pixels in the vascular invasion properties in cervical cancer, a set of system features was created by extending the ROI’s MBR from 10 to 60 pixels in all directions on the X1<sub>DCE</sub> MRI images. Different pixels with three patches up to the ROI of the MBR were created for a single MRI image, and they were used as training examples using EL models. With X1<sub>DCE</sub> MRI data and the EL model, Figure 12 represent the confusing matrix separation among non-vessel invasion and vessel invasion.

Compared to the AUC values achieved by utilizing the similar models training with pixels of 10 and 60 from the MBR of the original ROIs, the model of EL was training with pixels image enlarged by 30 pixels from the ROI, which reached the largest AUC. Table 2 predicts the EL approach performance evaluation with different patches. These

findings indicate that the cervical cancer, peri-tumor region plays a significant part in the ultimate classification of vascular invasion. The effect was thought to be explained by the following: The rapid growth of microorganisms inside the cancer before the invasion of the vessel causes the microvascular tumor to expand into neighboring tissues and cause small morphological changes in these tissues. Radiologists can sense design in surrounding tissues only depending on the regional scale features determined via visual inspection, and these current convolutional neural network algorithms can detect pixel-level properties and detect certain connections between morphological and pathological characteristics.

By combining predictive outcomes from both the X1<sub>DCE</sub> and X2<sub>WI</sub> MRI datasets, the structure of the recommended groups improved the predictive performance. This technique was inspired by the fact that radiologists make diagnostic decisions based on a thorough examination of several methods. These findings indicate the presence of careful group methods as a potential method for integrating

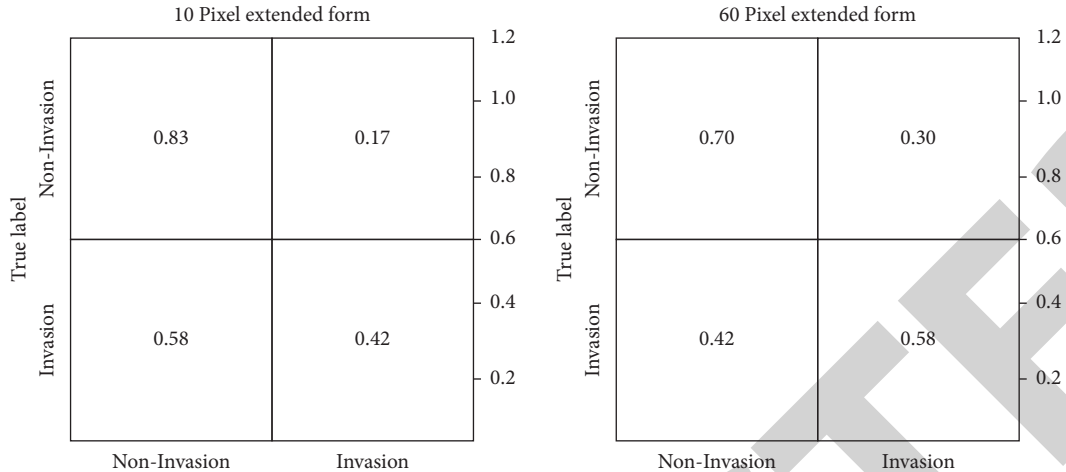


FIGURE 12: Confusion matrix assessment for vessel and non-vessel invasion.

TABLE 2: Various CNN model performance evaluation [ $A_c$  = Accuracy;  $S_n$  = Sensitivity;  $S_p$  = Specificity].

Various methods	ROC curve	$A_c$	$S_n$	$S_p$
AdaptiveVGG19 X1 <sub>DCE</sub>	0.79	0.75	0.65	0.78
AdaptiveVGG16 X1 <sub>DCE</sub>	0.82	0.68	0.74	0.75
AdaptiveInceptionV3/X1 <sub>DCE</sub>	0.78	0.81	0.85	0.65
AdaptiveVGG16/X2 <sub>WI</sub>	0.85	0.68	0.88	0.60
AdaptiveResNet50-V2/X1 <sub>DCE</sub>	0.89	0.78	0.68	0.87
AdaptiveInceptionV3/X2 <sub>WI</sub>	0.92	0.69	0.66	0.88
AdaptiveResNet50-V2/X2 <sub>WI</sub>	0.88	0.80	0.70	0.92
AdaptiveDenseNet121/X2 <sub>WI</sub>	0.87	0.88	0.72	0.77
AdaptiveDenseNet121/X1 <sub>DCE</sub>	0.92	0.77	0.87	0.84
AdaptiveVGG19-SE/X2 <sub>WI</sub>	0.89	0.85	0.79	0.82
AdaptiveVGG19-SE/X1 <sub>DCE</sub>	0.94	0.89	0.88	0.88
AdaptiveVGG19-CBAM/X2 <sub>WI</sub>	0.85	0.91	0.82	0.89
AdaptiveVGG19-CBAM/X1 <sub>DCE</sub>	0.90	0.87	0.79	0.88
Proposed A-EL/X1 <sub>DCE</sub> + X2 <sub>WI</sub>	0.95	0.96	0.91	0.94

TABLE 3: Different pixel performance evaluation.

Pixels expansion	AUC	$A_c$	$S_n$	$S_p$
Pixel range 10	0.78	0.77	0.56	0.89
Pixel range 30	0.90	0.89	0.92	0.97
Pixel range 60	0.88	0.65	0.97	0.78

multiframetric MRI databases into diagnostic and therapeutic applications. Furthermore, CNN-based radiomic systems are modifiable. As a result, new information classification assumptions can be provided utilizing a pre-trained framework with previously defined dependencies, weights, and other parameters that appear convenient and useful to facilitate the work. This is another important reason why detectives used CNN networks to complete this task Table 3.

## 5. Conclusion

Utilizing multi-parametric MRI data, this research presents in-depth radiomic approaches that may differentiate

between non-vessel invasion and vessel invasion in cervical cancer. Specifically, the research focuses on vessel invasion.

These findings provide evidence that comprehensive neurological network-based radiomics techniques are able to accurately forecast vascular invasion in cervical cancer that is in its early stages. In addition, these methods do not call for time-consuming human operations such as manual division, the construction of features, or selection.

By utilizing a method known as focused group learning, we were able to achieve a high level of prediction accuracy. This method possesses a significant amount of potential and a great deal of promise for use in supporting future clinical applications.

## Data Availability

The data used to support the findings of this study are included in the article. Further data or information is available from the corresponding author upon request.

## Conflicts of Interest

The authors declare that there are no conflicts of interest regarding the publication of this paper.

## Acknowledgments

The authors appreciate the supports from St. Joseph University, Tanzania for the research and preparation of the manuscript. The authors thank to Nitte Meenakshi Institute of Technology, Northwestern University, for providing assistance to complete this work. This project was supported by Researchers Supporting Project number (RSP-2021/283) King Saud University, Riyadh, Saudi Arabia.

## References

- [1] J. H. Shepherd, "Cervical cancer," *Best Practice & Research Clinical Obstetrics & Gynaecology*, vol. 26, no. 3, pp. 293–309, 2012.

- [2] H. H. Chung, B. H. Nam, J. W. Kim et al., "Preoperative [18F] FDG PET/CT maximum standardized uptake value predicts recurrence of uterine cervical cancer," *European Journal of Nuclear Medicine and Molecular Imaging*, vol. 37, no. 8, pp. 1467–1473, 2010.
- [3] M. A. El-Nashar, R. Y. Bamjboor, A. Algethami, B. A. alhomaiani, A. Alfaqeeh, and B. Althobaity, "Awareness of the women about the vaginal infection as a risk factor for cervical cancer in Taif city, Saudi Arabia," *International Journal of Medicine in Developing Countries*, vol. 4, no. 12, p. 2108, 2020.
- [4] K. Patel-Lippmann, J. B. Robbins, L. Barroilhet, B. Anderson, E. A. Sadowski, and J. Boyum, "MR imaging of cervical cancer," *Magnetic Resonance Imaging Clinics of North America*, vol. 25, no. 3, pp. 635–649, 2017.
- [5] L. A. Torre, F. Bray, R. L. Siegel, J. Ferlay, J. Lortet-Tieulent, and A. Jemal, "Global cancer statistics, 2012," *CA: A Cancer Journal for Clinicians*, vol. 65, no. 2, pp. 87–108, 2015.
- [6] H. K. Pannu, F. M. Corl, and E. K. Fishman, "CT evaluation of cervical cancer: spectrum of disease," *RadioGraphics*, vol. 21, no. 5, pp. 1155–1168, 2001.
- [7] S Orlhac, F. Chargari, C. Nioche et al., "Prediction of cervical cancer recurrence using textural features extracted from 18F-FDG PET images acquired with different scanners," *Oncotarget*, vol. 8, no. 26, pp. 43169–43179, 2017.
- [8] M. Fang, Y. Kan, D. Dong et al., "Multi-habitat based radiomics for the prediction of treatment response to concurrent chemotherapy and radiation therapy in locally advanced cervical cancer," *Frontiers in Oncology*, vol. 10, p. 563, 2020.
- [9] R. Banik, S. Naher, M. Rahman, and D. Gozal, "Investigating Bangladeshi rural women's awareness and knowledge of cervical cancer and attitude towards HPV vaccination: a community-based cross-sectional analysis," *Journal of Cancer Education*, vol. 37, no. 2, pp. 449–460, 2020.
- [10] H. J. W. L. Aerts, "The potential of radiomic-based phenotyping in precision medicine," *JAMA Oncology*, vol. 2, no. 12, pp. 1636–1642, 2016.
- [11] Y. Q. Huang, Ch Liang, L. He et al., "Development and validation of a radiomics nomogram for preoperative prediction of lymph node metastasis in colorectal cancer," *Journal of Clinical Oncology*, vol. 34, no. 18, pp. 2157–2164, 2016.
- [12] Y. Kan, D. Dong, Y. Zhang et al., "Radiomic signature as a predictive factor for lymph node metastasis in early-stage cervical cancer," *Journal of Magnetic Resonance Imaging*, vol. 49, no. 1, pp. 304–310, 2019.
- [13] J. Chen, B. He, D. Dong et al., "Noninvasive CT radiomic model for preoperative prediction of lymph node metastasis in early cervical carcinoma," *British Journal of Radiology*, vol. 93, no. 1108, Article ID 20190558, 2020.
- [14] A. Jajodia, A. Gupta, H. Prosch et al., "Combination of radiomics and machine learning with diffusion-weighted MR imaging for clinical outcome prognostication in cervical cancer," *Tomography*, vol. 7, no. 3, pp. 344–357, 2021.
- [15] U. K. Lilhore, M. Poongodi, A. Kaur et al., "Hybrid model for detection of cervical cancer using causal analysis and machine learning techniques," *Computational and Mathematical Methods in Medicine*, vol. 2022, pp. 1–17, 2022.
- [16] Y. R. Park, Y. J. Kim, W. Ju, K. Nam, S. Kim, and K. G. Kim, "Comparison of machine and deep learning for the classification of cervical cancer based on cervicography images," *Scientific Reports*, vol. 11, no. 1, pp. 1–11, 2021.
- [17] N. A. Mayr, T. Taoka, W. T. Yuh et al., "Method and timing of tumor volume measurement for outcome prediction in cervical cancer using magnetic resonance imaging," *International Journal of Radiation Oncology, Biology, Physics*, vol. 52, no. 1, pp. 14–22, 2002.
- [18] R. Vidya and G. M. Nasira, "Prediction of cervical cancer using hybrid induction technique: a solution for human hereditary disease patterns," *Indian Journal of Science and Technology*, vol. 9, no. 30, pp. 1–10, 2016.
- [19] R. Alsmariy, G. Healy, and H. Abdelhafez, "Predicting cervical cancer using machine learning methods," *International Journal of Advanced Computer Science and Applications*, vol. 11, no. 7, pp. 173–184, 2020.
- [20] M. Sharma, "Cervical cancer prognosis using genetic algorithm and adaptive boosting approach," *Health Technology*, vol. 9, no. 5, pp. 877–886, 2019.
- [21] M. M. Ali, K. Ahmed, F. M. Bui et al., "Machine learning-based statistical analysis for early stage detection of cervical cancer," *Computers in Biology and Medicine*, vol. 139, Article ID 104985, 2021.
- [22] S. Jahan, M. D. S. Islam, L. Islam et al., "Automated invasive cervical cancer disease detection at early stage through suitable machine learning model," *SN Applied Sciences*, vol. 3, no. 10, pp. 1–17, 2021.
- [23] Y. Xu, L. Zhu, B. Liu et al., "Strain elastography imaging for early detection and prediction of tumor response to concurrent chemo-radiotherapy in locally advanced cervical cancer: feasibility study," *BMC Cancer*, vol. 17, no. 1, pp. 427–429, 2017.